Author(s): Tanskanen, E. I. & Pulkkinen, Tuija I. & Viljanen, A. & Mursula, K. & Partamies, N. & Slavin, J. A.

Title: From space weather toward space climate time scales: Substorm analysis from 1993 to 2008

Year: 2011

Version: Final published version

Please cite the original version:

Tanskanen, E. I. & Pulkkinen, Tuija I. & Viljanen, A. & Mursula, K. & Partamies, N. & Slavin, J. A. 2011. From space weather toward space climate time scales: Substorm analysis from 1993 to 2008. Journal of Geophysical Research: Space physics, Vol. 116, nro A00I34. P. 10. ISSN 0148-0227 (printed). DOI: 10.1029/2010JA015788.

From space weather toward space climate time scales: Substorm analysis from 1993 to 2008

E. I. Tanskanen,[1,2] T. I. Pulkkinen,[3] A. Viljanen,[1] K. Mursula,[4] N. Partamies,[1] and J. A. Slavin[5]

Received 14 June 2010; revised 5 January 2011; accepted 13 January 2011; published 3 May 2011.

[1] Magnetic activity in the Northern Hemisphere auroral region was examined during solar cycles 22 and 23 (1993–2008). Substorms were identified from ground-based magnetic field measurements by an automated search engine. On average, 550 substorms were observed per year, which gives in total about 9000 substorms. The interannual, seasonal and solar cycle-to-cycle variations of the substorm number (R_{ss}), substorm duration (T_{ss}), and peak amplitude (A_{ss}) were examined. The declining phases of both solar cycles 22 and 23 were more active than the other solar cycle phases due to the enhanced solar wind speed. The spring substorms during the declining solar cycle phase ($|A_{ss,decl}| = 500$ nT) were 25% larger than the spring substorms during the ascending solar cycle years ($|A_{ss,acs}| = 400$ nT). The following seasonal variation was found: the most intense substorms occurred during spring and fall, the largest substorm frequency in the Northern Hemisphere winter, and the longest-duration substorms in summer. Furthermore, we found a winter-summer asymmetry in the substorm number and duration, which is speculated to be due to the variations in the ionospheric conductivity. The solar cycle-to-cycle variation was found in the yearly substorm number and peak amplitude. The decline from the peak substorm activity in 1994 and 2003 to the following minima took 3 years during solar cycle 22, while it took 6 years during solar cycle 23.

Citation: Tanskanen, E. I., T. I. Pulkkinen, A. Viljanen, K. Mursula, N. Partamies, and J. A. Slavin (2011), From space weather toward space climate time scales: Substorm analysis from 1993 to 2008, *J. Geophys. Res.*, *116*, A00I34, doi:10.1029/2010JA015788.

1. Introduction

[2] Auroral oval magnetic activity has been examined visually over several hundred years [see *Siscoe*, 1980]. Ground-based magnetic observatories set up around the globe have made continuous scientific observations of the auroral processes possible. For a long time, auroral oval activity, e.g., substorms, were identified and analyzed manually or semi-manually. Only recently, analysis methods and techniques have developed to the level that enable studies over several years and solar cycles. Space weather observations begin to turn to space climate observations when the time series expand to cover several tens of years and several solar cycles.

[3] The terrestrial magnetosphere is rarely in a quiet state when no storms, substorms, or other types of geomagnetic activity is in progress. Most of the time, large or small geomagnetic changes occur in many locations and altitudes in the magnetosphere and ionosphere. The southern and northern auroral regions are activated almost every day because of internal disturbances in the ionosphere and the external disturbances of solar and solar wind origin. Typically one to four auroral substorms occur daily [*Kamide*, 1982; *Borovsky et al.*, 1993]. The substorm duration varies from 1 to 5 h [*Kullen and Karlsson*, 2004]; some storm time substorms may last several hours longer.

[4] Quantitative results of substorm properties vary slightly depending on how the individual substorms have been identified and on the data set that has been used. Substorms can be identified from either space-borne or ground-based observations. Space-borne substorm observations can be done, e.g., at the geostationary orbit, in the magnetotail lobes or from polar-orbiting spacecraft. On the ground, substorm signatures have usually been sought from auroral keograms, all-sky camera images, or magnetograms. When substorms are identified from magnetograms, the typical substorm duration is about 3 h [*Tanskanen*, 2009]. Substorm signatures measured in the magnetotail [*Slavin et al.*, 1984; *Miyashita et al.*, 2003], at the geostationary orbit [*Rosenqvist et al.*, 2002; *Liou et al.*, 1999] or in the polar orbit [*Pulkkinen et al.*, 1997], have shorter duration than the magnetic signatures measured on ground.

[1]Finnish Meteorological Institute, Helsinki, Finland.
[2]Department of Physics and Technology, University of Bergen, Bergen, Norway.
[3]School of Electrical Engineering, Aalto University, Aalto, Finland.
[4]Department of Physics, University of Oulu, Oulu, Finland.
[5]NASA Goddard Space Flight Center, Greenbelt, Maryland, USA.

0148-0227/11/2010JA015788

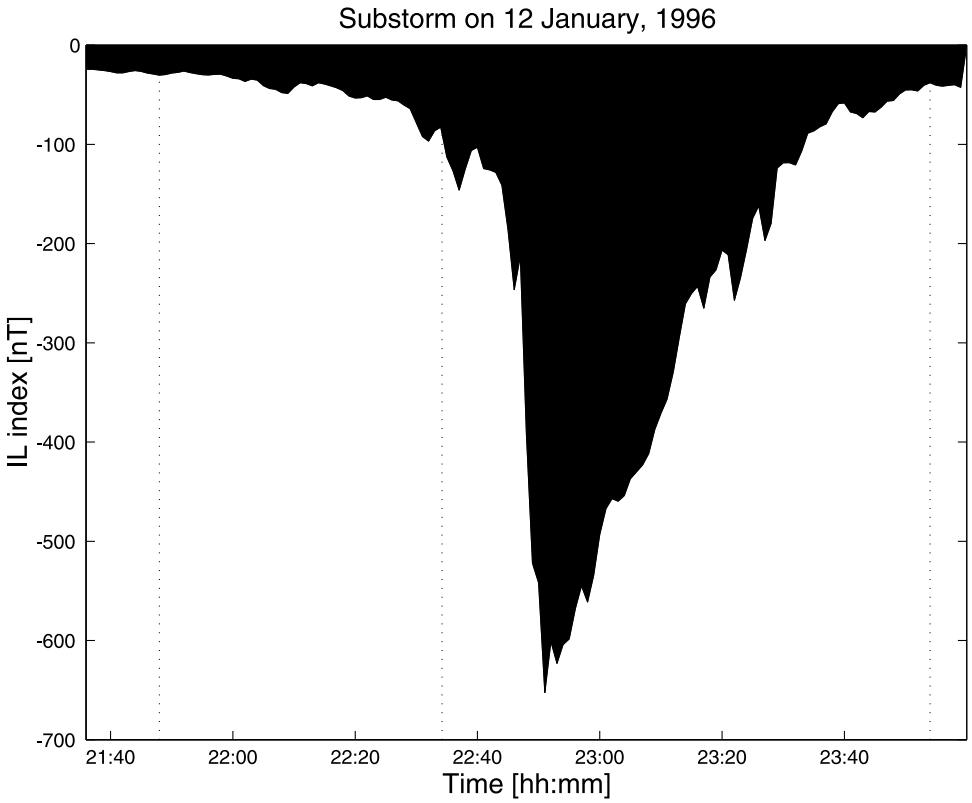

Figure 1. IL index for a typical medium-sized substorm on 12 January 1996, starting at 2210 UT. The peak amplitude of 652 nT was reached at the Svalbard and Bear Island stations.

[5] One of the earliest patterns recognized in geomagnetic activity is the semiannual variation [*Cortie*, 1912; *Chapman and Bartels*, 1940]. The auroral region is known to behave differently during the equinoctial months than around solstices. The semiannual variation appears as spring and fall maxima in various geomagnetic activity indices [*Russell and McPherron*, 1973] and in individual substorm studies [*Tanskanen*, 2009]. The average peak amplitude has been observed to be larger for the spring and fall substorms than for the winter and summer substorms [*Tanskanen*, 2009].

[6] The interannual and solar cycle-to-cycle variation of geomagnetic activity has been examined in the auroral region [*Nevanlinna and Pulkkinen*, 1998] and at midlatitudes [*Caan et al.*, 1978] by using time series of several activity indices. The longest available data set of visual auroral observations covers about 500 years [*Silverman*, 1992]. Visual aurora observations and the westward electrojet index in the IMAGE local time sector are known to show solar cycle dependence [*Nevanlinna and Pulkkinen*, 1998]. *Nevanlinna and Pulkkinen* [1998] argued that the auroral occurrence, at least near the equatorward edge of the standard oval, correlates with the level of solar activity. A data set of substorms over a complete solar cycle, 1993–2003, has been analyzed by *Tanskanen et al.* [2005a] and by *Tanskanen* [2009]. The substorm number and intensity were shown to contain a clear solar cycle dependence such that both parameters closely track the interplanetary high-speed stream activity.

[7] The Sun is the origin for most of geomagnetic disturbances observed at the Earth. The Sun goes through an 11 year solar cycle. During a solar minima most of the sunspots are found in latitude bands around 30 degrees from the solar equator, from where the sunspot populations in each hemisphere migrate to low latitudes close to the equator. The sunspot maximum is often double-spiked with a less active Gnevyshev gap [*Gnevyshev*, 1963, 1977] in between. The size and duration of the Gnevyshev gap varies from one solar cycle to another. As the solar activity progresses through the 11 year cycle, the characteristic disturbances associated with the solar activity vary: The highly geoeffective magnetic clouds and coronal mass ejections are observed more often during solar maximum than during other solar cycle phases [e.g., *Gopalswamy et al.*, 2008; *Lepping et al.*, 2006], while the declining solar cycle phases are dominated by high-speed streams [*Holzer and Slavin*, 1981; *Tanskanen et al.*, 2005a].

[8] The Sun-borne geoeffective structures are transported via the solar wind toward the Earth, where they cause geomagnetic disturbances in many parts of the magnetosphere. Interplanetary shocks and coronal mass ejections are known to cause the most abrupt and dramatic changes in geomagnetic activity [e.g., *Gopalswamy et al.*, 2008; *Huttunen et al.*, 2005; *Tsurutani et al.*, 2010], while other drivers, e.g., corotating interaction region (CIR) related high-speed streams (HSS), are known to drive the magnetosphere more smoothly over long time intervals up to several weeks [*Tsurutani et al.*, 2006]. The connection between the solar wind and geomagnetic disturbances has been characterized by coupling functions. Coupling functions are typically a combination of a solar wind bulk velocity, interplanetary magnetic field

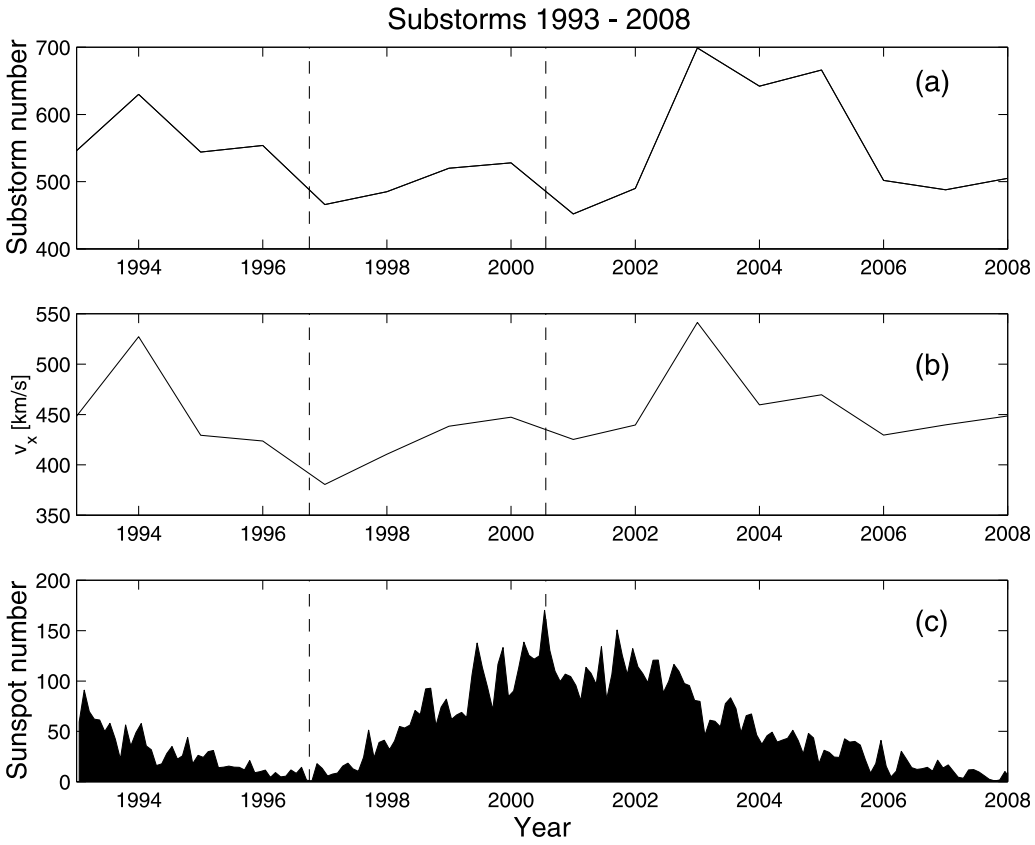

Figure 2. (a) Interannual variation of the substorm number from 1993 to 2008. The average yearly substorm number is 517 with a standard deviation of 75. The substorm number and (b) the yearly averaged solar wind velocity reaches maximum in 1994 and 2003. (c) The solar activity maximum defined by the sunspot number is in 2000 and the minimum is in 1996. The sunspot minimum and maximum are marked with vertical dotted lines in all three panels.

intensity, and its southward component, possibly added with or replaced by other variables such as the IMF clock angle or solar wind plasma density [*Perreault and Akasofu*, 1978; *Akasofu*, 1981; *Holzer and Slavin*, 1982].

[9] In this paper, we identify and examine substorms based on ground-based magnetic observations from 1993 to 2008, covering the declining phase of solar cycle 22 and the entire solar cycle 23. We present the interannual (section 3), seasonal (section 4) and solar cycle-to-cycle variation (section 5) of the substorm number (R_{ss}), duration (T_{ss}), and peak amplitude (A_{ss}). In section 6 we discuss possible causes for the observed variations in the different time scales.

2. Substorm Database

[10] Magnetic field measurements from the IMAGE network between 56° and 76° geomagnetic latitudes and between 96° and 112° geomagnetic longitudes are used to identify substorms. Magnetic observatories in this longitude range rotate across local midnight between 1600 and 0300 UT, when the network can be used to detect substorm signatures in the nightside auroral region [*Kauristie et al.*, 1996]. By using a dense network with a good latitudinal coverage, it is possible to detect the true peak amplitude of substorms and the true occurrence frequency covering also smaller events which might be missed by the global indices based on less dense observational network. The IMAGE ground-based magnetic field measurements give a high-quality data covering several solar cycles.

[11] We identified and examined all substorms in the IMAGE data in the time interval between 1600 and 0300 UT each day over one and half solar cycles from 1993 to 2008. Solar cycle 23 began in May 1996 and peaked in April 2000, while solar cycle 22 started in September 1986 and peaked in August 1990. The IL index [*Kallio et al.*, 2000] is created from the measurements of about 15–28 IMAGE observatories between 1993 and 2008 [*Viljanen and Häkkinen*, 1997; *Syrjäsuo et al.*, 1998] in the northern auroral region. The IL index is the envelope curve of the north-south component of the magnetic field computed in the similar way to the Kyoto AL index.

[12] In total, 8717 substorms were identified from the IL index by using a high-throughput search engine described in detail by *Tanskanen* [2009]. While substorms show highly variable characteristics, for the purpose of statistical analysis over several years and solar cycles, a mechanistic substorm definition is needed. The substorm identification scheme is as follows: The main substorm onset was sought by searching a rapid decrease in the IL index exceeding 80 nT in 15 min, leading to a negative bay development. The substorm was defined to begin when the first sign of the negative bay developed (IL index changes from quiet level

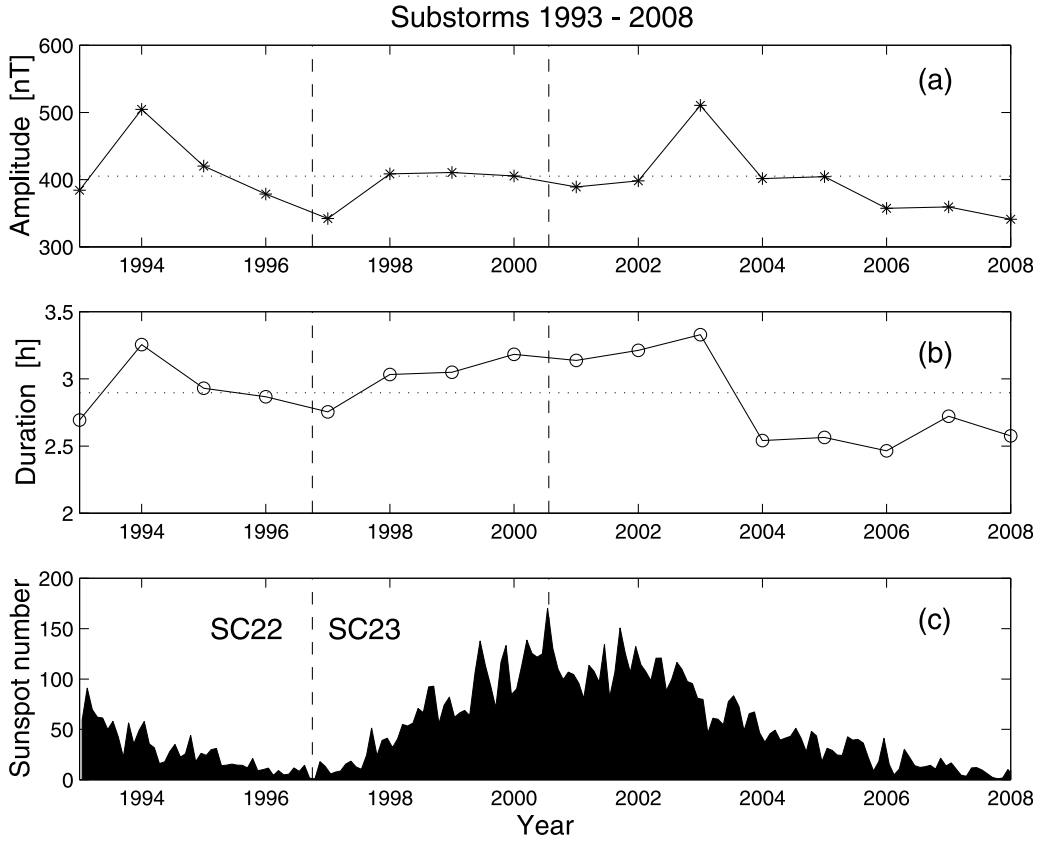

Figure 3. (a) Interannual variation of the substorm peak amplitude and (b) duration from 1993 to 2008. The mean values for amplitude (405 nT) and duration (2 h and 55 min) are shown with a horizontal dotted line. The standard deviation of the peak amplitude is 48 nT and 17 min for a duration. Substorms are smaller and shorter at the end of the solar cycle 23 compared to the substorms in all other years. The strongest and longest substorms are found in 1994 and 2003 during a declining solar cycle phase. As a comparison, (c) the monthly averaged sunspot number is shown.

values close to zero to the disturbed state values). The substorm was defined to end when the IL index returned to 20% of the peak substorm amplitude. The search engine technique has been evaluated and, for example, the use of a limited UT interval was tested [*Tanskanen*, 2009]. We ran the search engine for different UT intervals and found that the trend for substorm number and peak amplitude holds.

[13] We show a typical substorm on 12 January 1996 in Figure 1. The substorm started at 2150 UT with a slow and smooth growth from −20 nT down to −100 nT during the growth phase. The weak growth phase signatures of the substorm were first observed over mainland Finland at the Oulujärvi station (64.52° geographic latitude, 27.23° geographic longitude). The substorm expanded northward in 17 min, reaching a peak amplitude of 652 nT. The clearest substorm signal (a negative bay with a sharp decrease) was observed over Svalbard and Bear Island stations. The duration of the entire substorm was about 2 h 5 min, which was clearly less than the average substorm duration of the entire data set (3 h).

3. Interannual Substorm Variations

[14] The interannual substorm variations were examined by computing yearly averages of the substorm number, substorm duration, and peak amplitude. Figure 2 shows the annual substorm numbers from 1993 to 2008 (R_{ss} = 546, 630, 544, 554, 466, 485, 520, 528, 452, 490, 699, 642, 666, 502, 488, 505), the annually averaged solar wind bulk speed, and the monthly averaged sunspot number for the same years. The average substorm number for this data set was 517 per year with a standard deviation of 75. The largest substorm numbers were observed in 1994 ($R_{ss,1994}$ = 630), 2003 ($R_{ss,2003}$ = 699), 2004 ($R_{s,2004}$ = 642), and 2005 ($R_{ss,2005}$ = 666). All these years with substorm number exceeding 600 occur during the declining phase of the solar cycle. Figure 2 shows that the substorm number does not follow the sunspot number, but the largest substorm numbers are observed few years after the solar maximum during the declining solar cycle phase. Small substorm numbers around 450 were observed as well during a sunspot minimum (e.g., year 1997) as during a sunspot maximum (e.g., year 2001). The substorm number for the year 2001 ($R_{ss,2001}$ = 452) was smallest in this data set, being about 20% smaller than the average. The minimum in 2001 occurred around the time of the Gnevyshev gap in solar activity. Note that the substorm number never decreased to below 450. Even when the solar activity was very low, the terrestrial auroral region was active and auroral substorms still occurred frequently.

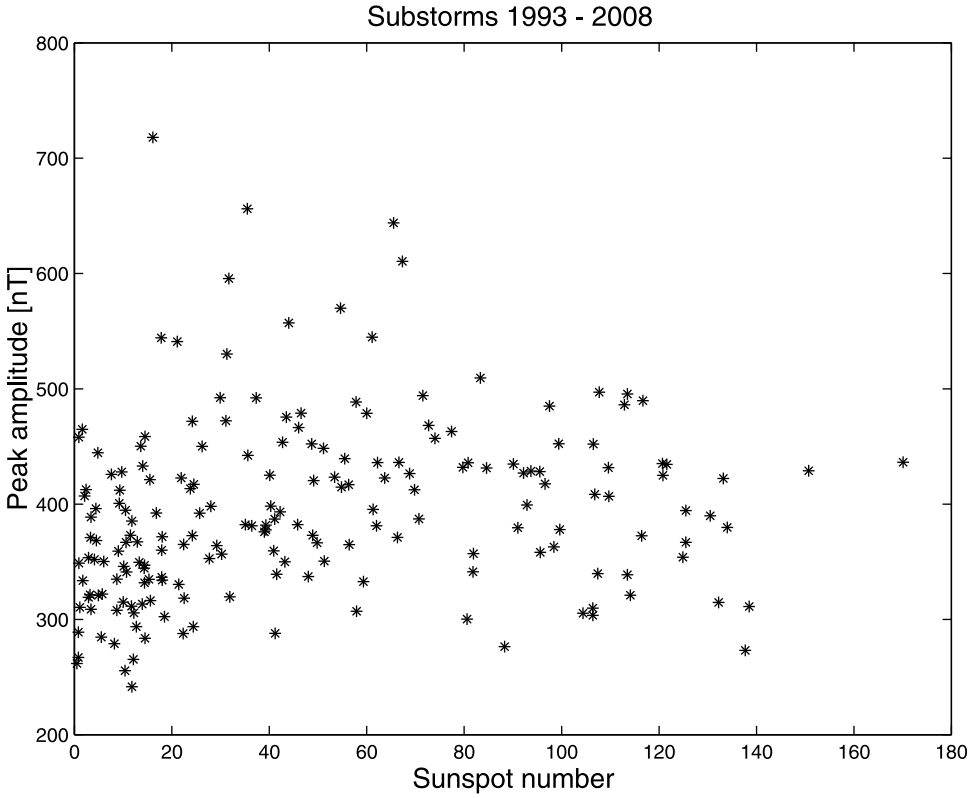

Figure 4. A monthly substorm peak amplitude as a function of the sunspot number in 1993–2008. The linear correlation coefficient for the sunspot number and the peak amplitude is as low as 0.17.

[15] Comparison of the solar wind velocity with the substorm number in Figure 2 shows a clear connection. The rule-of-the thumb can be formulated in the following way: When the yearly averaged solar wind speed is about 450 km/s, the yearly averaged substorm number is about 400 (low solar activity case), and when the yearly averaged solar wind speed is about 550 km/s, then the substorm number is about 500 (high solar activity case).

[16] Yearly averaged substorm peak amplitudes are shown in Figure 3. The average peak amplitude was about 400 nT with the standard deviation of 48 nT. The 2 years with the strongest substorms, on average, were 1994 and 2003, when the yearly averaged peak amplitude was 500 nT and 510 nT, respectively. The 2 years with the smallest peak amplitudes occurred in 1997 ($A_{ss,1997}$ = 342 nT) and 2008 ($A_{ss,2008}$ = 341 nT). The yearly averaged peak amplitudes did not follow the sunspot number, but the peak amplitude maximum was delayed for about 2–4 years from the sunspot maximum. Figure 4 shows a scatterplot, where the x axis gives the sunspot number and the y axis gives the substorm peak amplitude. The linear correlation coefficient for the sunspot number and the peak amplitude is 0.17. Thus, the substorm peak amplitude cannot be predicted on the basis of the sunspot number. For example, the typical substorm of 400 nT could occur during any sunspot number from close to zero up to 170. However, the substorm peak amplitude in Figure 3a clearly follows the yearly velocity values in Figure 2b. The linear correlation coefficient between the yearly averaged solar wind speed and the yearly averaged substorm peak amplitude is 0.9 over one solar cycle (1993–2003) and 0.8 for the entire data set (1993–2008).

[17] The substorm duration varied from tens of minutes to several hours. The average substorm duration for the data set was about 3 h with a 17 min standard deviation. The longest-duration substorms were observed in 1994 (T_{ss} = 3 h 15 min) and 2003 (T_{ss} = 3 h 20 min). The shortest-duration substorms were detected at the end of solar cycle 23, from 2004 to 2008, when the yearly averaged substorm duration was around 2.5 h.

4. Seasonal Variation

[18] The peak amplitude of all substorms in 1996 are shown to demonstrate the seasonal variation (Figure 5). The year 1996 marks the end of the declining phase of the solar cycle 22, just prior to solar minimum. The peak amplitude of the substorms in 1996varied between 210 nT and 1852 nT, while their duration varied from 48 min to several hours. The substorm number for 1996 is $R_{ss,1996}$ = 554, and the average size of the substorms is $A_{ss,1996}$ = 380 nT.

[19] The seasonal substorm variation was examined by computing the monthly substorm number and the monthly average of the duration and peak amplitude for the entire data set. We found that substorms occur less frequently in the Northern Hemisphere summer than in spring, fall, or winter months. Figure 6a shows the seasonal variation of the monthly substorm number averaged over the entire 16 year interval. The monthly substorm occurrence rate is about two times larger in winter than during the summer months. The trend of having less substorms during the summer months than during other months holds for all examined years. Another illustration of the winter-summer asymmetry is the

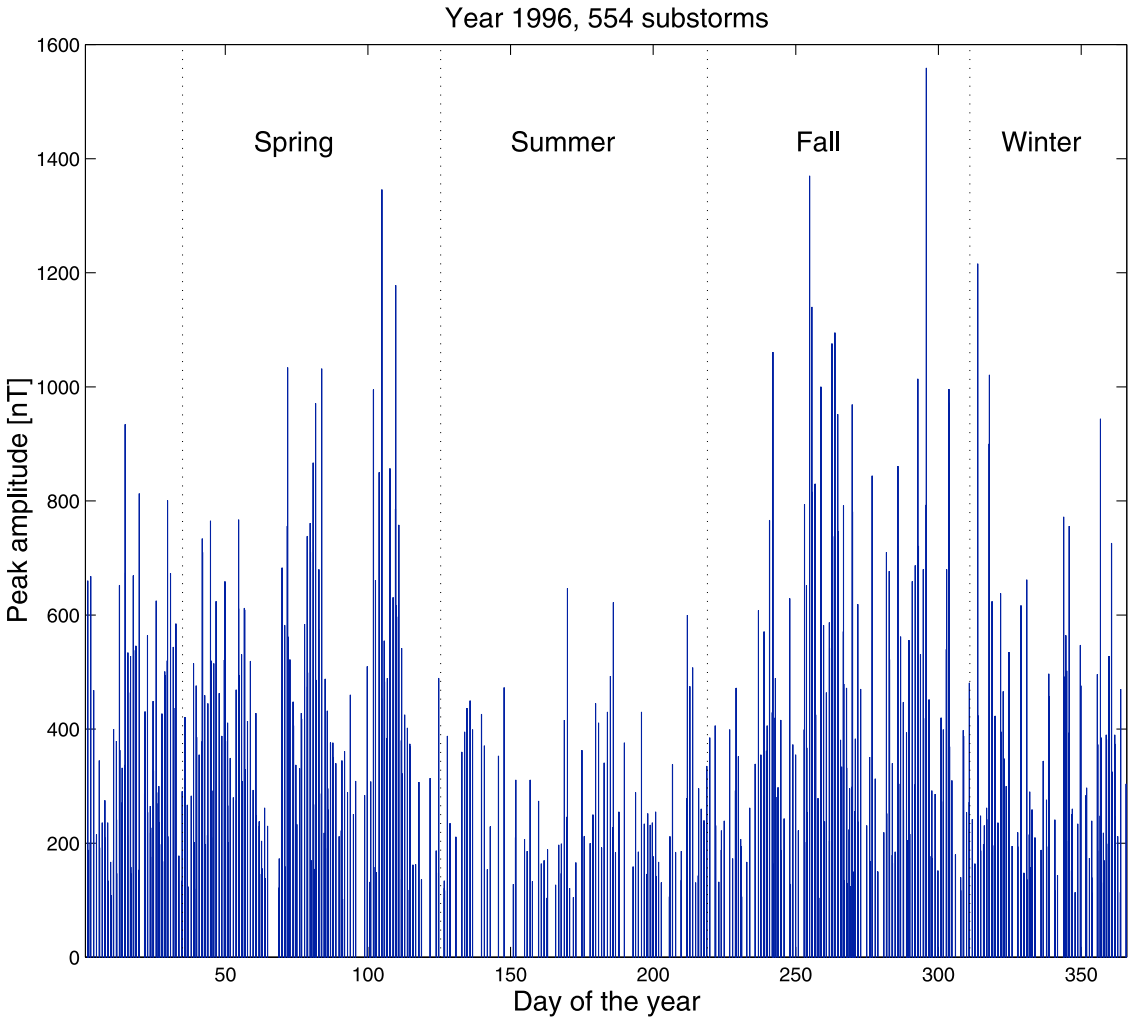

Figure 5. The peak amplitudes for all 554 substorms in 1996. Spring, summer, fall, and winter months are separated from each other by vertical dotted lines. The Northern Hemisphere summer substorms in 1996 are weaker than substorms in other seasons.

winter-summer asymmetry in substorm duration. The substorm duration has its maximum during summer months (Figure 6b). Summer substorms last about 3.5 h, while winter substorms last on average an hour less.

[20] Figure 6c shows the seasonal variation of the substorm peak amplitude. The monthly substorm peak amplitude has its maximum typically in spring and fall, as expected. However, the shape of the monthly substorm peak amplitude curve is not symmetric between spring and fall. The enhancement is broader in spring than in fall, but the peak amplitudes are slightly larger during fall than spring. When plotting the monthly peak amplitude curve separately for each year, we found that during certain years the spring maximum was larger than the fall maximum, and vice versa in other years. A more detailed analysis is given at the end of section 5 (see Figure 9).

5. Comparison of Solar Cycles 22 and 23

[21] The solar cycle variation in the substorm number, duration, and peak amplitude was examined by comparing substorms detected during solar cycle 22 to the substorms of the solar cycle 23. Our data set includes substorm observations during the entire solar cycle 23 (years 1997–2008) and during the declining phase of the solar cycle 22 (years 1993–1996). We will compare the substorms of the two declining phases to each other and briefly compare the substorms of the ascending solar cycle phase 23 (years 1997–2000) to the substorms of the declining solar cycle phase 22 (years 1993–1996).

[22] The solar cycles 22 and 23 show very similar features: (1) The largest substorm numbers and peak amplitudes were observed during the declining solar cycle phases (in 1994 and 2003), and (2) the lowest-peak amplitudes occurred during the solar minimum. One of the main differences between cycles 22 and 23 was that the return time from the highest activity in 1994 and in 2003 to the lowest activity took 3 years during the cycle 22, while it took 6 years during the cycle 23.

[23] The seasonal variations of the monthly substorm number, duration, and peak amplitude were compared during the declining phases of the solar cycle 22 (1993–1996) and 23 (2004–2008) (Figure 7). The substorm number and duration show very similar trends during both solar cycles.

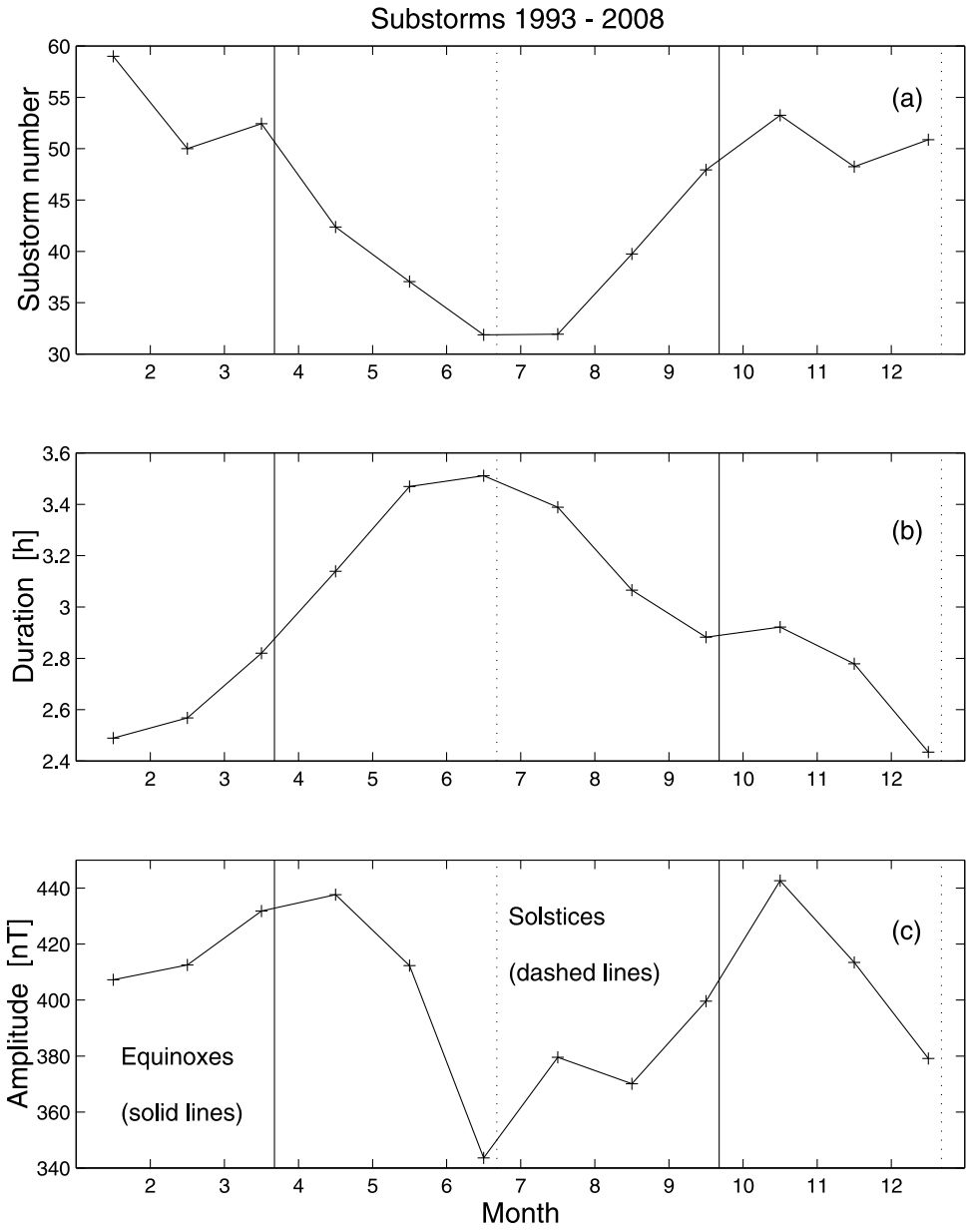

Figure 6. Average seasonal variation of (a) monthly substorm number, (b) substorm duration, and (c) substorm peak amplitude for the entire data set of 8717 substorms. Equinoxes are shown with a straight vertical line and solstices with a dashed vertical line.

The monthly substorm number reached minimum in the summer (Figure 7a), and the duration reached minimum in the winter (Figure 7b). However, the trend in the substorm peak amplitude varied from one solar cycle to the next. During the decline of the cycle 22, the peak amplitude showed pronounced spring and fall maxima, which were only weakly present during the decline of the solar cycle 23. The pattern for the cycle 23 was different because there were several additional active months, which were not present in the cycle 22. For example, January and July were active in 2004–2006. The seasonal variation during 2003, which was the most active year in the entire data set, was examined separately because of its extreme characteristics. The year 2003 showed a typical seasonal variation in the substorm number and duration, but the peak amplitude showed some atypical features (Figure 8). The most notable is the large fall maximum, which was delayed from the fall equinox. There was a slight additional increase in activity around spring equinox and in May. The unusual active months may be due to the few highly active events that were disturbing the terrestrial auroral magnetosphere in 2003 (e.g., substorms during the Halloween storm from the end of October to the beginning of November).

[24] The seasonal variation of the substorm peak amplitude was examined separately during the declining (1993–1996) and ascending (1997–2000) solar cycles phases (Figure 9). The substorms during the declining and during the ascending solar cycle phases seem to have some similarities but also some differences. The monthly peak amplitude curves have a similar shape during the declining and

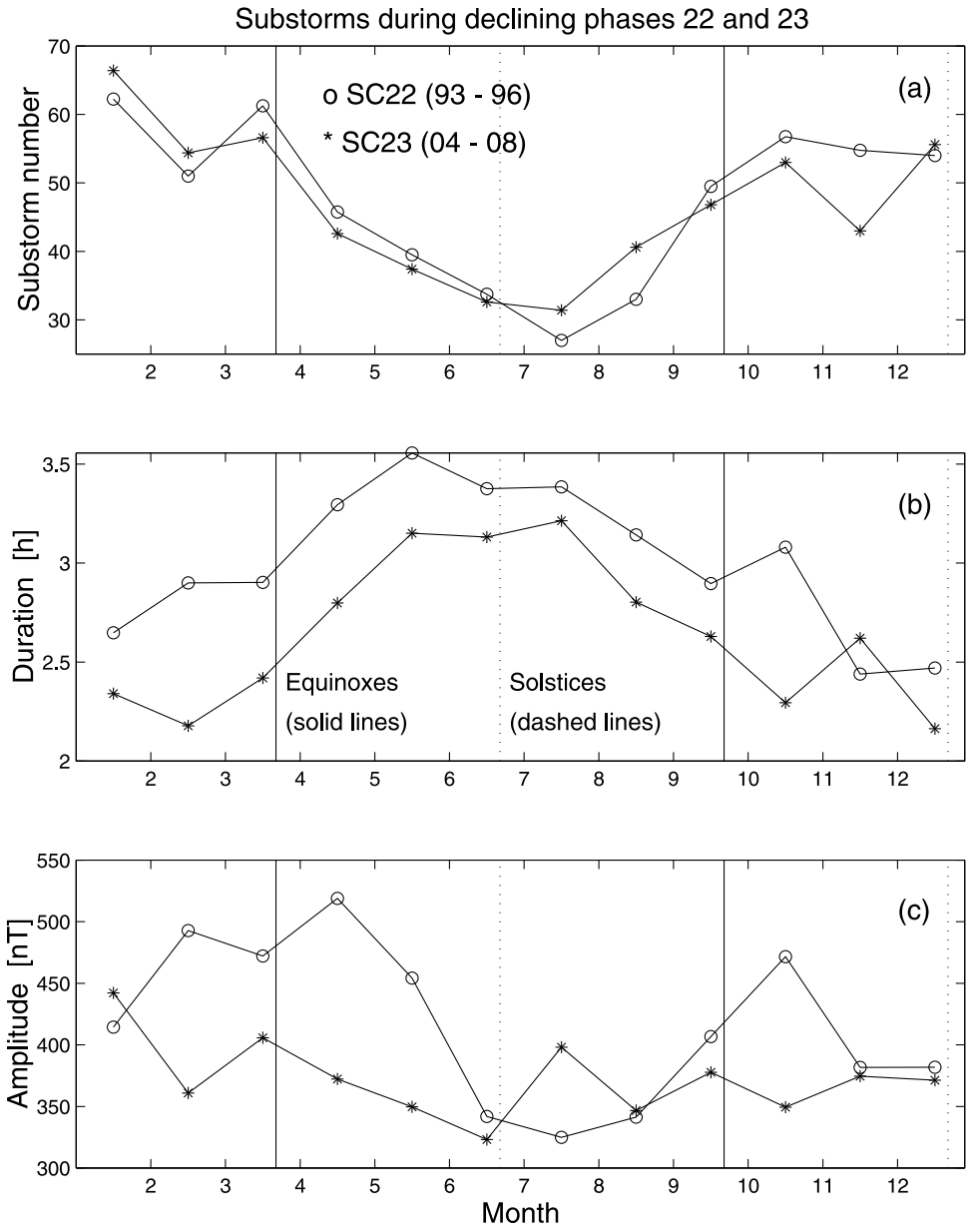

Figure 7. Average seasonal variation of (a) monthly substorm number, (b) duration, and (c) peak amplitude during the declining solar cycle phases 22 and 23. Declining phase of the solar cycle 22 (marked by circles) includes years from 1993 to 1996, and declining phase 23 (marked by asterisks) includes years from 2004 to 2008.

ascending phases. The activity maxima occur during equinoxes and the minima occur during summer solstice. Furthermore, the spring activity peaks seem to be double-peaked and "broader" than the single-peaked fall activity. The main difference between the declining and ascending solar cycle phases was that spring substorms during the declining solar cycle phase($A_{ss,decl}$ = 500 nT) were 25% larger than spring substorms during the ascending solar cycle years ($|A_{ss,incl}|$ = 400 nT). Furthermore, spring substorms were more intense during the declining solar cycle phase, while fall substorms were more intense during the ascending solar cycle phase. Consequently, the entire Northern Hemisphere auroral region is more active during the declining than the ascending solar cycle phase, but the seasonal variation of the substorm number and duration (e.g., the winter-summer asymmetry) is independent of the solar cycle phase.

6. Discussion

[25] Magnetospheric substorms over one and half solar cycles (1993–2008) have been examined. Substorm properties vary with both season and solar cycle. The two declining (cycles 22 and 23) and one inclining (cycle 23) solar cycle phases are covered by the examined substorm data set of about 9000 substorms. The role of interplanetary and ionospheric sources of the observed variation will be discussed.

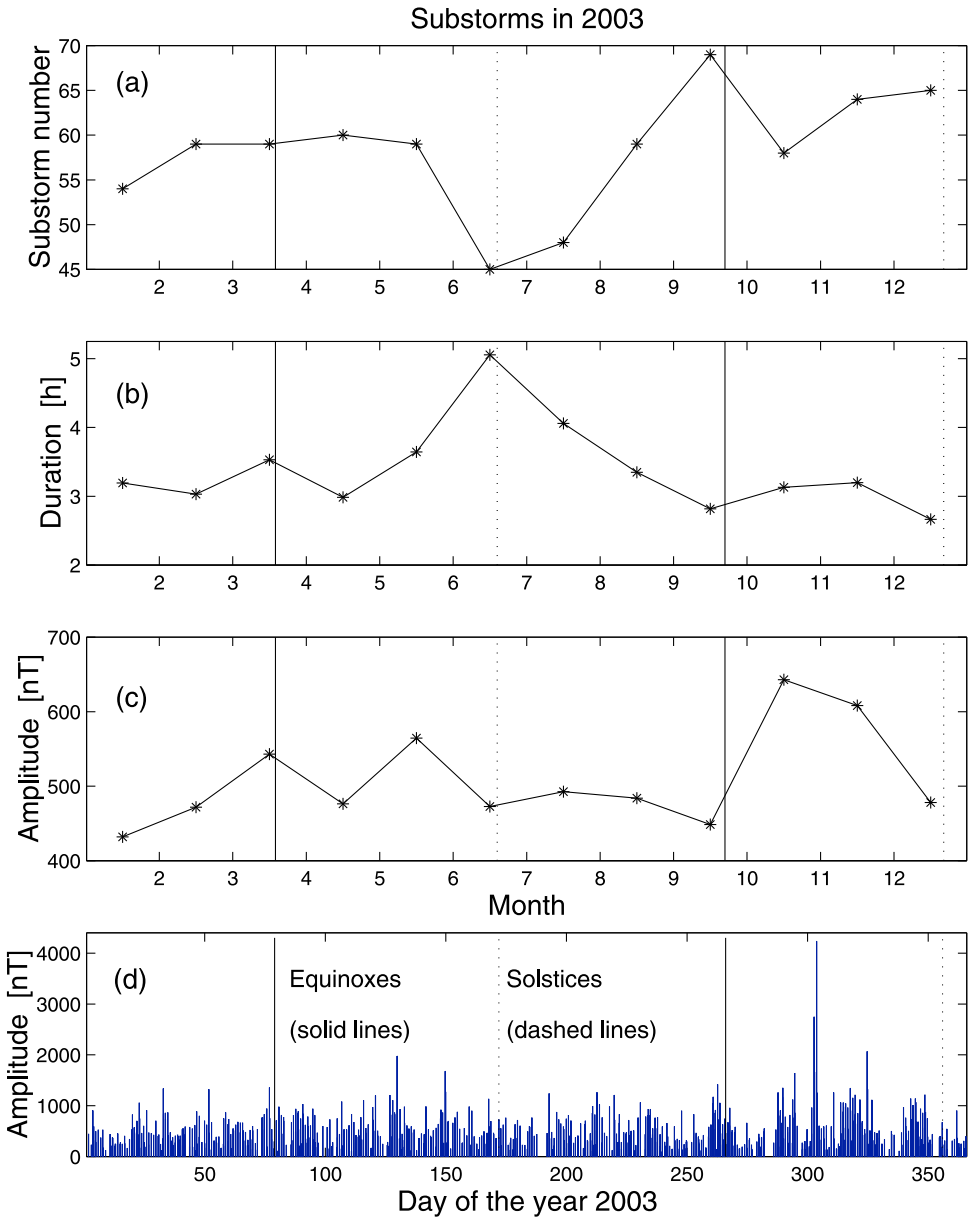

Figure 8. Average seasonal variation of (a) monthly substorm number, (b) duration, and (c) peak amplitude in 2003. (d) The peak amplitudes of all substorms in 2003 are shown. The year 2003 is extremely active, including few extremely strong substorms in October.

[26] Several interplanetary plasma properties are shown to vary over the years [e.g., *Intriligator*, 1975]. For example, solar cycle variations of the interplanetary magnetic field [*Svalgaard and Wilcox*, 1975; *Emery et al.*, 2009], solar wind velocity [*Newkirk*, 1983], density [*Richardson et al.*, 2000; *Crooker et al.*, 2000], and helium abundance [*Ogilvie and Hirshberg*, 1974; *Aellig et al.*, 2001] have been reported. Furthermore, the interaction of the solar wind with the terrestrial magnetosphere [*Bai and Sturrock*, 1993] as well as with the other planets [*Slavin et al.*, 1979] has been shown to show annual variations. Three main explanations for the seasonal variations are (1) axial hypothesis, (2) equinoctial hypothesis, and (3) Russell-McPherron effect. The axial hypothesis relates the changes in the heliographic latitude of the Earth during the year to the annual changes in geomagnetic activity [*Cortie*, 1912], while in the equinoctial hypothesis, the driver is the solar wind flow direction variations with respect to the Earth's magnetic dipole axis [*Bartels*, 1925; *McIntosh*, 1959]. The Russell-McPherron effect associates the seasonal variation with the variation of the angle between the geocentric solar magnetospheric (GSM) equatorial plane and the solar equatorial plane [*Russell and McPherron*, 1973]. None of the three main causes alone, or any combination of them, can explain completely the observed seasonal variation of magnetospheric storms [*Häkkinen et al.*, 2003; *Cliver et al.*, 2000] or radiation belt energetic electrons [*Kanekal et al.*, 2010; *Vassiliadis et al.*, 2002]. The complete set of processes causing the

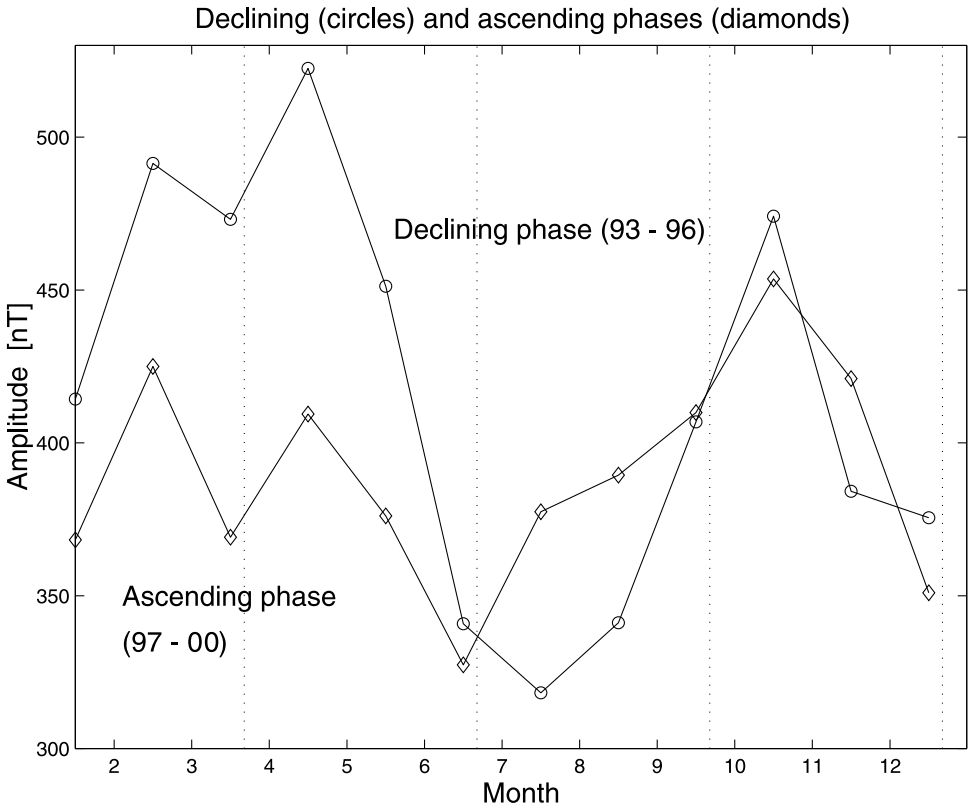

Figure 9. Average seasonal variation of the substorm peak amplitude during the declining solar cycle phase 22 (circles) and during the ascending solar cycle phase 23 (diamonds). Spring substorms during the declining solar cycle phase 22 are 25% larger than spring substorms during the ascending solar cycle phase 23.

semiannual variation is still an open question, after more than 150 years after the discovery of the phenomenon.

[27] We found the largest number of substorms in winter during the declining solar cycle phase, the longest substorms in summer during sunspot maxima, and the most intense substorms in spring and fall during the declining solar cycle phase. The occurrence and intensity maxima during the declining solar cycle phase are mainly due to the solar wind driving conditions. Long-lasting high-speed solar wind streams enhance terrestrial geomagnetic activity [*Holzer and Slavin*, 1981; *Guarniera et al.*, 2006; *Despirak et al.*, 2007] and substorm activity in particular [*Tanskanen et al.*, 2005a]. High-speed streams are known to be good drivers for auroral substorms, providing smooth, long-lasting driving together with frequent negative IMF B_z intervals [*Tanskanen et al.*, 2005b]. The winter-summer asymmetry in the substorm occurrence is most likely due to variable ionospheric conditions. The ionospheric conductivity in the Northern Hemisphere where the IMAGE network is located is largest in summer and smallest in winter. The smaller conductivity in winter time may decrease the substorm trigger level and increase the number of substorms, as suggested by *Wang and Lühr* [2007]. The longer duration of the summer substorms may indicate that the substorms have time to recover completely before the next substorm begins. In winter conditions, substorms occur more frequently, and the substorm recovery is more often interrupted by the next substorm. This hypothesis needs to be tested with future investigations.

[28] During the sunspot maxima the interplanetary space is filled with shocks, coronal mass ejections, flux ropes, and other drivers for geomagnetic storms. These structures are present in the solar wind about 37% of the time during a solar maximum and only 5% of the time during a solar minimum [*Emery et al.*, 2009]. This means that during sunspot maxima, the entire magnetosphere is in a highly disturbed state during at least one third, or even one half, of the time, and auroral oval activity is affected by the storm activity. Previous studies show that the storm time substorms differ from their nonstorm time counterparts [*Tanskanen et al.*, 2002]: for example, the storm time substorms last about 10% longer than nonstorm substorms [*Tanskanen*, 2002]. This can be speculated to explain the increase in the substorm length around solar maximum such that more storm time substorms occur during sunspot maximum than during the other solar cycle phases [*Karinen and Mursula*, 2005].

[29] The most intense substorms in this data set were detected during spring and fall, which agrees well with the equinoctial maxima of geomagnetic activity in general [*Sabine*, 1852; *Cortie*, 1912]. The semiannual variation is argued not to be simply due to the creation of the southward component of the interplanetary magnetic field during equinoxes (i.e., mountain building, which means increased

coupling) [*Cliver et al.*, 2000] but primarily because of the loss of coupling efficiency during the solstices (i.e., valley digging, which means decreased coupling) [*Cliver et al.*, 2000]. The spring-fall asymmetry during the ascending solar cycle phase, which is reported in this paper (Figure 9), agrees well with previous studies showing larger electron fluxes [*Vassiliadis et al.*, 2002] and stronger storms [*Häkkinen et al.*, 2003] during fall than spring. Furthermore, the fall response is reported to last longer compared to the spring response [*Holzer and Slavin*, 1981]. That agrees with our result of getting about 10 min longer substorms in fall than spring. *Häkkinen et al.* [2003] found that for the Southern Hemisphere, the spring-fall asymmetry (as well as the winter-summer asymmetry) is opposite; stronger storms were observed in spring than fall (and summer than winter). In this paper, the spring substorms during the declining solar cycle phase were found to be more intense than the fall substorms, opposite to the observed spring-fall asymmetry during the ascending solar cycle phase (Figure 9). We speculate that a possible reason for that is the difference between the response of the oval disturbances (i.e.,substorms) and equatorial magnetic disturbances (i.e., storms) to the enhanced high-speed stream activity.

7. Summary of Main Results

[30] The main results of the study are the following:

[31] 1. We found interannual variations in the substorm number, duration, and peak amplitude. The declining phases of solar cycles 22 and 23 were more active than other solar cycle phases mostly because of the enhanced solar wind speeds. A rule-of-the-thumb between solar wind speed and substorm activity is that a low substorm activity (400 substorms per year) is connected to a low solar wind speed (450 km/s), and a high substorm activity (500 substorms per year) is connected to a solar wind speed averaging about 500 km/s.

[32] 2. The substorm number was smallest in 2001 ($R_{ss,2001}$ = 452), about 20% smaller than the average. Furthermore, the substorm number and peak amplitude were smaller than average around sunspot minima in 1996, 1997, and 2008.

[33] 3. The substorm number and duration show very similar seasonal trends during both solar cycles 22 and 23. The substorm number reached minimum in the Northern Hemisphere summer, and the duration reached minimum in winter. However, the trend in the substorm peak amplitude varied from one solar cycle to the next. During the declining cycle 22, the peak amplitude showed pronounced spring and fall maxima, which were only weakly present during the declining phase of the solar cycle 23. Furthermore, recovery from the peak substorm activity in 1994 and 2003 took 3 years during the solar cycle 22, while it took 6 years during the cycle 23.

[34] 4. A winter-summer asymmetry was found for the substorm number and substorm duration. During the winter months, the substorm number was about two times larger than during the summer months, but summer substorms were about an hour longer than their winter counterparts.

[35] 5. The main difference between the declining and ascending solar cycle phase was that substorms during the declining phase were larger than during the ascending solar cycle years. The spring substorms during the declining solar cycle phase ($|A_{ss,decl}|$ = 500 nT) were 25% larger than during ascending solar cycle years ($|S_{ss,incl}|$ = 400 nT). Furthermore, the fall maxima were larger than the spring maxima during the ascending solar cycle phase and vice versa for the declining phase.

[36] **Acknowledgments.** We wish to thank the institutes maintaining the IMAGE magnetometer network. The work of E.T. was funded by Academy project 108518 and by Ministry of Transport and Communications in Finland. Furthermore, K.M. and E.T. acknowledge the financial support by the Academy of Finland to the HISSI research consortium projects 128189 and 128632.

[37] Philippa Browning thanks Anita Kullen and another reviewer for their assistance in evaluating this paper.

References

Aellig, M. R., A. J. Lazarus, and J. T. Steinberg (2001), The solar wind helium abundance: Variation with wind speed and the solar cycle, *Geophys. Res. Lett.*, *28*, 2767.

Akasofu, S.-I. (1981), Energy coupling between the solar wind and the magnetosphere, *Space Sci. Rev.*, *28*, 121.

Bai, T., and P. A. Sturrock (1993), Evidence for a fundamental period of the Sun and its relation to the 154 day complex of periodities, *Astrophys. J.*, *409*, 476.

Bartels, J. (1925), Eine universelle Tagesperiode der erdmagnetischen Aktivität, *Meteorol. Z.*, *42*, 147.

Borovsky, J. E., R. J. Nemzek, and D. Belian (1993), The occurrence rate of magnetospheric substorm onsets: Random and periodic substorms, *J. Geophys. Res.*, *98*, 3807.

Caan, M. N., R. L. McPherron, and C. T. Russell (1978), The statistical magnetic signatures of magnetospheric substorms, *Planet. Space Sci.*, *26*, 269–279, doi:10.1016/0032-0633(78)90092-2.

Chapman, S., and J. Bartels (1940), *Geomagnetism*, vol. 1, chapter 11, Oxford Univ. Press, New York.

Cliver, E. W., Y. Kamide, and A. G. Ling (2000), Mountains versus valleys: Semiannual variation of geomagnetic activity, *J. Geophys. Res.*, *105*, 2413.

Cortie, A. L. (1912), Sunspots and terrestrial magnetic phenomena, 1898–1911: The cause of the annual variation in magnetic disturbances, *Mon. Not. R. Astron. Soc.*, *73*, 52.

Crooker, N. U., S. Shodhan, J. T. Gosling, J. Simmer, R. P. Lepping, J. T. Steinberg, and S. W. Kahler (2000), Density extremes in the solar wind, *Geophys. Res. Lett.*, *27*, 3769.

Despirak, I. V., A. A. Lubchich, A. G. Yahnin, and B. V. Kozelov (2007), The influence of high-speed solar wind streams on the auroral bulge parameters, in *Physics of Auroral Phenomena, Proc. XXX Annual Seminar, Apatity*, pp. 21–25, Polar Geophys. Inst., Apatity, Russ.

Emery, B. A., I. G. Richardson, D. S. Evans, and F. J. Rich (2009), Solar wind structure sources and periodities of auroral electron power over three solar cycles, *J. Atmos. Sol. Terr. Phys.*, *71*, 1157.

Gnevyshev, M. N. (1963), The corona and the 11-year solar cycle of solar activity, *Sov. Astron., Engl. Transl.*, *7*, 311.

Gnevyshev, M. N. (1977), Essential features of the 11-year solar cycle, *Sol. Phys.*, *51*, 175.

Gopalswamy, N., S. Akiyama, S. Yashiro, G. Michalek, and R. P. Lepping (2008), Solar sources and geospace consequences of interplanetary magnetic clouds during solar cycle 23, *J. Atmos. Sol. Terr. Phys.*, *70*, 245.

Guarniera, F. L., B. T. Tsurutani, E. Echer, and W. D. Gonzalez (2006), Geomagnetic activity and auroras caused by high-speed streams: A review, in *Advances in Geosciences: Solar Terrestrial*, vol. 8, edited by M. Duldig et al., p. 91, World Sci., Hackensack, N. J.

Häkkinen, L. V. T., T. I. Pulkkinen, R. J. Pirjola, H. Nevanlinna, E. I. Tanskanen, and N. E. Turner (2003), Seasonal and diurnal variation of geomagnetic activity: Revised Dst versus external drivers, *J. Geophys. Res.*, *108*(A2), 1060, doi:10.1029/2002JA009428.

Holzer, R. E., and J. A. Slavin (1981), The effect of solar wind structure on magnetospheric energy supply during solar cycle 20, *J. Geophys. Res.*, *86*, 675.

Holzer, R. E., and J. A. Slavin (1982), An evaluation of three predictors of geomagnetic activity, *J. Geophys. Res.*, *87*, 2558.

Huttunen, K. E. J., R. Schwenn, V. Botmer, and H. E.J. Koskinen (2005), Properties and geoeffectiveness of magnetic clouds in the rising, maximum and early declining phases of solar cycle 23, *Ann. Geophys.*, *23*, 625.

Intriligator, D. S. (1975), The solar cycle variation in the solar wind and the modulation of cosmic rays, in *International Conference on X-rays in Space* (*Cosmic, Solar and Auroral X-rays*), *the University of Calgary, Calgary, Alberta, August* 14–21, 1974, vol. 3, p. 1033, Univ. of Calgary, Calgary, Alberta, Canada.

Kallio, E. I., T. I. Pulkkinen, H. E. J. Koskinen, and A.Viljanen (2000), Loading-unloading processes in the nightside ionosphere, *Geophys. Res. Lett.*, *27*, 1627.

Kamide, Y. (1982), Two-component aurora electrojet, *Geophys. Res. Lett.*, *9*, 1175.

Kanekal, S. G., D. N. Baker, and R. L. McPherron (2010), On the seasonal dependency of relativistic electron fluxes, *Ann. Geophys.*, *28*, 1101.

Karinen, A., and K. Mursula (2005), A new reconstruction of the Dst index for 1932–2002, *Ann. Geophys.*, *23*, 475.

Kauristie, K., T. I. Pulkkinen, R. J. Pellinen, and H. J. Opgenoorth (1996), What can we tell about the AE-index from a single meridional magnetometer chain?, *Ann. Geophys.*, *14*, 1177.

Kullen, A., and T. Karlsson (2004), On the relation between solar wind, pseudobreakups, and substorms, *J. Geophys. Res.*, *109*, A12218, doi:10.1029/2004JA010488.

Lepping, R. P., D. B. Berdichevsky, C.-C. Wu, A. Szabo, T. Naroc, F. Mariani, A. J. Lazarus, and A. J. Quivers (2006), A summary of WIND magnetic clouds for years 1995–2003: Model-fitted parameters, associated errors and classifications, *Ann. Geophys.*, *24*, 215.

Liou, K., C.-I. Meng, T. Y. Lui, P. T. Newell, M. Brittnacher, G. Parks, G. D. Reeves, R. R. Anderson, and K. Yumoto (1999), On relative timing in substorm onset signatures, *J. Geophys. Res.*, *104*, 22,807.

McIntosh, D. H. (1959), On the annual variation of magnetic disturbances, *Philos. Trans. R. Soc. London, Ser. A*, *251*, 525.

Miyashita, Y., S. Machida, K. Liou, T. Mukai, Y. Saito, H. Hayakawa, C.-I. Meng, and G. K. Parks (2003), Evolution of the magnetotail associated with substorm auroral breakups, *J. Geophys. Res.*, *108*(A9), 1353, doi:10.1029/2003JA009939.

Nevanlinna, H., and T. I. Pulkkinen (1998), Solar cycle correlation of substorm and auroral occurrence frequency, *Geophys. Res. Lett.*, *16*, 3087.

Newkirk, G., Jr. (1983), Solar cycle variation of the latitudinal gradient of solar wind speed, *Bull. Am. Astron. Soc.*, *15*, 699.

Ogilvie, K. W., and J. Hirshberg (1974), The solar cycle variation of the solar wind helium abundance, *J. Geophys. Res.*, *79*, 4595.

Perreault, P., and S.-I. Akasofu (1978), A study of geomagnetic storms, *Geophys. J. R. Astron. Soc.*, *54*, 547.

Pulkkinen, T. I., et al. (1997), Solar wind-magnetosphere coupling during an isolated substorm event: A multispacecraft ISTP study, *Geophys. Res. Lett.*, *24*, 983.

Richardson, I. G., D. Berdichevsky, M. D. Desch, and D. J. Farrugia (2000), Solar-cycle variation of low density solar wind during more than three solar cycles, *Geophys. Res. Lett.*, *27*, 3761.

Rosenqvist, L., E. Borälv, and H. J. Opgenoorth (2002), Timing of substorm onset signatures on the ground and at geostationary orbit, *Geophys. Res. Lett.*, *29*(12), 1592, doi:10.1029/2001GL013939.

Russell, C. T., and R. L. McPherron (1973), Semiannual variation of geomagnetic activity, *J. Geophys. Res.*, *78*, 92.

Sabine, E. (1852), On periodical laws discoverable in the mean effects of the larger magnetic disturbances, *Philos. Trans. R. Soc. London*, *142*, 103.

Silverman, S. M. (1992), Secular variation of the aurora for the past 500 years, *Rev. Geophys.*, *30*, 333.

Siscoe, G. L. (1980), Evidence in the auroral record for secular solar variability, *Rev. Geophys.*, *18*, 647.

Slavin, J. A., R. C. Elphic, and C. T. Russell (1979), Pioneer-Venus magnetometer observations: Evidence for solar cycle variation in the solar wind interaction with Venus, *Bull. Am. Astron. Soc.*, *12*, 536.

Slavin, J. A., E. J. Smith, B. T. Tsurutani, D. G. Sibeck, H. J. Singer, D. N. Baker, J. T. Gosling, E. W. Hones, and F. L. Scarf (1984), Substorm associated traveling compression regions in the distant tail: ISEE-3 observations, *Geophys. Res. Lett.*, *11*, 657.

Svalgaard, L., and J. M. Wilcox (1975), Long-term evolution of solar sector structure, *Sol. Phys.*, *41*, 461.

Syrjäsuo, M., et al. (1998), Observations of substorm electrodynamics using the MIRACLE network, in *Substorms-4: International Conference on Substorms-4, Lake Hamana, Japan, March* 9–13, 1998, edited by S. Kokobun and Y. Kamide, p. 111, Terra Sci., Tokyo.

Tanskanen, E. I. (2002), Terrestrial substorms as a part of global energy flow, Ph.D. dissertation, Univ. of Helsinki, Helsinki, Finland.

Tanskanen, E. I. (2009), A comprehensive high-throughput analysis of substorms observed by IMAGE magnetometer network: Years 1993–2003 examined, *J. Geophys. Res.*, *114*, A05204, doi:10.1029/2008JA013682.

Tanskanen, E. I., T. I. Pulkkinen, H. E. J. Koskinen, and J. A. Slavin (2002), Substorm energy budget near solar minimum and maximum: 1997 and 1999 compared, *J. Geophys. Res.*, *107*(A6), 1086, doi:10.1029/2001JA900153.

Tanskanen, E. I., J. A. Slavin, A. Tanskanen, A. Viljanen, T. I. Pulkkinen, H. E. J. Koskinen, A. Pulkkinen, and J. Eastwood (2005a), Magnetospheric substorms are strongly modulated by interplanetary high-speed streams, *Geophys. Res. Lett.*, *32*, L16104, doi: 10.1029/2005GL023318.

Tanskanen, E. I., J. A Slavin, D. H. Fairfield, D. G. Sibeck, J. Gjerloev, T. Mukai, T. Nagai, and A. Ieda (2005b), Magnetotail response to prolonged southward IMF B_z intervals: Loading, unloading, and continuous dissipation, *J. Geophys. Res.*, *110*, A03216, doi:10.1029/2004JA010561.

Tsurutani, B. T., et al. (2006), Corotating solar wind streams and recurrent geomagentic activity: A review, *J. Geophys. Res.*, *111*, A07S01, doi:10.1029/2005JA011273.

Tsurutani, B. T., G. S. Lakhina, O. P. Verkhoglyadova, W. D. Gonzalez, E. Echer, and F. L. Guarnieri (2010), A review of interplanetary discontinuities and their geomagnetic effects, *J. Atmos. Sol. Terr. Phys.*, *73*, 5, doi:10.1016/j.jastp.2010.04.001.

Vassiliadis, D., A. J. Klimas, S. G. Kanekal, D. N. Baker, and R. S. Weigel (2002), Long-term average, solar cycle, and seasonal response of magnetospheric energetic electrons to the solar wind speed, *J. Geophys. Res.*, *107*(A11), 1383, doi:10.1029/2001JA000506.

Viljanen, A., and L. Häkkinen (1997), Image magnetometer network, in *Satellite-Ground Based Coordination Sourcebook*, edited by M. Lockwood, M. N. Wild, and H. J. Opgenoorth, p. 111, Eur. Space Agency, Noordwijk, Neth.

Wang, H., and H. Lühr (2007), Seasonal-longitudinal variation of substorm occurrence frequency: Evidence for ionospheric control, *Geophys. Res. Lett.*, *34*, L07104, doi:10.1029/2007GL029423.

K. Mursula, Department of Physics, University of Oulu, Oulu FI-90014, Finland.

N. Partamies, E. I. Tanskanen, and A. Viljanen, Finnish Meteorological Institute, PO Box 503, Helsinki FI-00101, Finland. (eija.tanskanen@fmi.fi)

T. I. Pulkkinen, School of Electrical Engineering, Aalto University, PO Box 13000, FI-00076 Aalto, Finland.

J. A. Slavin, NASA Goddard Space Flight Center, Code 670, Greenbelt, MD 20771, USA.